

Precision measurement of electrical charge with optomechanically induced transparency

Jian-Qi Zhang,¹ Yong Li,^{2,*} Mang Feng,^{1,†} and Yi Xu^{3,4}

¹*State Key Laboratory of Magnetic Resonance and Atomic and Molecular Physics, Wuhan Institute of Physics and Mathematics, Chinese Academy of Sciences, Wuhan 430071, China*

²*Beijing Computational Science Research Center, Beijing 100084, China*

³*Laboratory of Photonic Information Technology, School for Information and Optoelectronic Science and Engineering, South China Normal University, Guangzhou 510006, China*

⁴*School of Physics and Electric Engineering, Guangzhou University, Guangzhou 510006, China*

(Dated: October 31, 2018)

We propose a potentially practical scheme to precisely measure the charge number of small charged objects by using optomechanically induced transparency (OMIT) in optomechanical systems. In contrast to conventional measurements based on noise backaction on optomechanical systems, our scheme presents an alternative way to detect the charge number exactly, by monitoring small deformation of the mechanical resonator sensitive to the charge number of nearby charged object. The relationship between the charge number and the OMIT window width is investigated and the feasibility of the scheme is justified by numerical simulation with currently available experimental values.

PACS numbers: 42.50.Wk, 46.80.+j, 41.20.Cv

I. INTRODUCTION

Precision measurement is one of the essential tasks in the study of modern physics. The (micro- or nano-) mechanical resonators (MRs) hold the promise for realizing precision measurements due to the possibility of presenting both classical and quantum properties [1, 2]. For measurements approaching quantum limit [3] with mechanical systems, we have to cool the MRs to their ground states and show obvious quantum behavior. Up to now, various methods for MR cooling have been proposed in optomechanical and electromechanical systems, such as feedback cooling [4–6], backaction sideband cooling [7–9], bang-bang cooling [10], electromagnetically induced transparency cooling [11], measurement-based cooling [12], and thermal light cooling [13], some of which have been achieved experimentally [14–19].

The precision measurement based on MRs can be classified by two kinds of systems, i.e., optomechanical and electromechanical systems. We focus in the present work on the optomechanical system, in which the precision measurements were usually carried out via the correlations between the output spectra and measured quantities based on reflected noise [3]. For example, precision measurement of displacement of the MR has been achieved with a factor of five times higher than standard quantum limit in optical output spectra [20], and a recent experimental report was published for displacement measurement of the MR beyond standard quantum limit [21].

The optomechanically induced transparency (OMIT) is a kind of induced transparency caused by radiation pressure to couple light to MR modes [23]. Recently, the OMIT in optomechanical system has been predicted theoretically [22–24] and also observed experimentally [23, 25–27]. However, the application of OMIT has not yet been fully explored. As far as we know, the proposed applications are only for slow light with OMIT controlling the speed of light [26] and for single photon router with OMIT to control the probe field in a single photon Fock state [28].

The aim of the present work is to detect the charge number of a small charged body via OMIT in an optomechanical and electrical system. The Coulomb interaction between a charged MR and a nearby charged body in such a hybrid system will modify both the steady-state position of the MR and the mean photon number in the cavity, which affect significantly the window width of the OMIT [22, 23]. As a result, the charge number of the charged object is possibly detected via monitoring the modified window width of the OMIT.

Our study shows that the window widths in some special regions of the OMIT vary with the charge number in a sensitive way, which makes it possible for a precision measurement of the charge number. We notice that previous ideas for ultra-sensitive measurements in opto-mechanical systems, e.g., cavity optomechanical magnetometer [29] and displacement measurement [20], are based on quantum noise backaction [3]. In contrast, the noise backaction is unnecessary in our case because the output intensity of the probe field is monitored via the OMIT based on the expectation of massive photons. Moreover, conventional MR electrometers, such as vibrating reed electrometers [30], are formed by movable and fixed electrodes, which can be used to measure the

*Corresponding author Email: liyong@csrc.ac.cn

†Corresponding author Email: mangfeng@wipm.ac.cn

Coulomb forces with variable capacitors. Limited by the extremely sensitive electricity, e.g., 0.12 nA current [31], however, the MR electrometers cannot measure the charge densities in tiny objects (e.g., < 6 nm [32]). In contrast, since optical measurements are usually more sensitive than electrical ones, our scheme in an optical way should work well even for detecting single charges in very small objects. Furthermore, our scheme makes use of the unique feature of optomechanical measurements which is considered to have higher sensitivity than electromechanical measurements [33].

Our system consisting of both an optomechanical system and a charged object is actually a cavity optoelectromechanical system, belonging to a currently active research area. For example, a recent idea for detecting electric gradient force was proposed by using a net dipole moment in a microtoroid [34, 35]. In comparison, our scheme using OMIT can be applied to measure weaker force since the net charge density on a metal surface can be much higher than the net dipole moment density in a semiconduction surface. Moreover, there was a proposal to measure displacements and forces by noise spectra [36]. Honestly speaking, our scheme based on the expectation of massive photons might not work better than in Ref. [36] (Concrete estimates will be given later in the section of Conclusion). But our focus is on the electric charge detection, which is a practical application of OMIT.

The paper is structured as follows: We present the model and Hamiltonian of the system in next section, and study the output field for the OMIT in Sec. III. The relationship between the charge number and the output field as well as the feasibility of our scheme is described in Sec. IV. The last section is for a brief conclusion.

II. MODEL AND HAMILTONIAN

The model we consider is sketched in Fig. 1, where a high-quality cavity consists of a fixed mirror and a movable one, i.e., a MR. Besides the radiation pressure force coupling the MR to the cavity mode, the charged MR is subject to the Coulomb force due to the charged body nearby. Such a system can be described as

$$H_1 = \hbar\omega_c c^\dagger c + \left(\frac{p^2}{2m} + \frac{m\omega_m^2}{2} q^2 \right) - \chi q c^\dagger c - \frac{n|e|Q_{MR}}{4\pi\epsilon(r_0 - q)} + i\hbar[(\epsilon_l e^{-i\omega_l t} + \epsilon_p e^{-i\omega_p t})c^\dagger - \text{H.c.}]. \quad (1)$$

Here the first term is for the single-mode cavity of eigen-frequency ω_c with the bosonic annihilation (creation) operator c (c^\dagger). The second term describes the vibration of the MR where q and p are, respectively, the position and momentum operators of the MR with eigen-frequency ω_m and effective mass m . The third term is for the radiation pressure coupling the cavity field to the MR, with $\chi = \hbar\omega_c/L$ the coupling strength and L being the cavity length. The fourth term presents the interaction of the

charged MR with the charged body via a Coulomb potential $V_c = \frac{-n|e|Q_{MR}}{4\pi\epsilon(r_0 - q)}$, where Q_{MR} is the positive charge on the MR, $-n|e|$ is for n negative charges of the charged body to be detected, and r_0 is the distance between the equilibrium positions of the MR center-of-mass and the charged body in absence of the radiation pressure and the Coulomb force. In our case with the attractive force, the Coulomb force on the MR points to the same direction as the radiation pressure force on the MR. The last term in Eq. (1) describes two optical drives to the cavity from the fixed mirror: One is the strong pumping field with frequency ω_l and the other is the weak probe field with frequency ω_p , and ϵ_l and ϵ_p are the corresponding driving strengths, respectively.

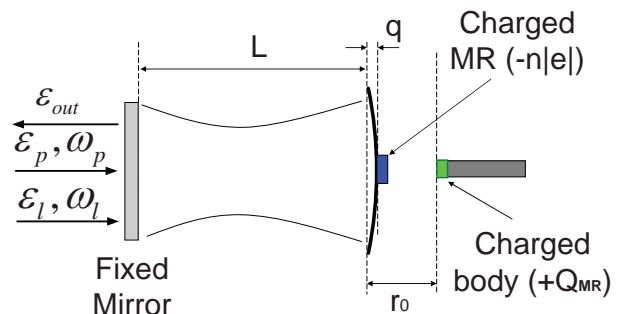


FIG. 1: Schematic diagram of the system. An optomechanical cavity with the length L is driven by two light fields. One is the pumping field ϵ_l with frequency ω_l and the other is the probe field ϵ_p with frequency ω_p . The output field is represented by ϵ_{out} . r_0 is the distance between the charged body and the charged MR in absence of the radiation pressure and the Coulomb force. Under the action of the radiation pressure and the Coulomb force, the MR takes a position q . Here, the charges on the charged body and charged MR are $-n|e|$ and Q_{MR} , respectively.

In the case of $q \ll r_0$, the Coulomb interaction can be rewritten as $V_c \simeq -\frac{n|e|Q_{MR}}{4\pi\epsilon r_0} \left(1 + \frac{q}{r_0}\right)$. Omitting the constant term, we have the Hamiltonian in the frame rotating with the driving frequency ω_l ,

$$H_2 = \hbar\Delta_c c^\dagger c + \frac{1}{2m}(p^2 + m^2\omega_m^2 q^2) - \chi q c^\dagger c - n\eta q + i\hbar[(\epsilon_l + \epsilon_p e^{-i\delta t})c^\dagger - \text{H.c.}], \quad (2)$$

where $\Delta_c = \omega_c - \omega_l$, $\eta = |e|Q_{MR}/(4\pi\epsilon r_0^2)$, and $\delta = \omega_p - \omega_l$. Here both ϵ_l and ϵ_p are complex.

III. MEAN-VALUE EQUATIONS AND QUADRATURES OF THE OUTPUT FIELD

For analyzing the mean response of the OMIT, we may consider the Langevin equations [37] by neglecting quantum fluctuation of the system [22]. In our case, the mean-

value equations of the system are written as,

$$\begin{aligned} \left\langle \frac{dq}{dt} \right\rangle &= \frac{\langle p \rangle}{m}, \\ \left\langle \frac{dp}{dt} \right\rangle &= -m\omega_m^2 \langle q \rangle + n\eta + \chi \langle c^\dagger c \rangle - \gamma_m \langle p \rangle, \\ \left\langle \frac{dc}{dt} \right\rangle &= -[\kappa + i(\Delta_c - \frac{\chi}{\hbar} \langle q \rangle)] \langle c \rangle + \varepsilon_l + \varepsilon_p e^{-i\delta t}, \end{aligned} \quad (3)$$

where κ and γ_m are introduced as the decay rates of the cavity and the MR, respectively. Eq. (3) can be solved under the condition that the pumping field is much stronger than the probe one. Eq. (3) is a nonlinear equation and the steady-state response in the frequency domain is composed of many frequency components. We suppose the steady-state solutions to Eq. (3) taking the form of

$$\begin{aligned} \langle q \rangle &= p_s + p_+ \varepsilon_p e^{-i\delta t} + p_- \varepsilon_p^* e^{i\delta t}, \\ \langle p \rangle &= q_s + q_+ \varepsilon_p e^{-i\delta t} + q_- \varepsilon_p^* e^{i\delta t}, \\ \langle c \rangle &= c_s + c_+ \varepsilon_p e^{-i\delta t} + c_- \varepsilon_p^* e^{i\delta t}, \end{aligned} \quad (4)$$

where each solution contains three items O_s , O_+ and O_- (with $O = p, q, c$), corresponding to the responses at the original frequencies ω_l , ω_p , and $2\omega_l - \omega_p$, respectively [37]. Since $O_s \gg O_\pm$, Eq. (4) can be solved by treating O_\pm as perturbation. After combining Eq. (4) with Eq. (3), and ignoring the second-order small terms, we obtain the steady-state mean-values of the system by resorting the prefactors in terms of the exponentials $e^{\pm i\delta t}$

$$\begin{aligned} p_s &= 0, & q_s &= \frac{\chi |c_s|^2 + n\eta}{m\omega_m^2}, \\ c_s &= \frac{\varepsilon_l}{\kappa + i\Delta}, & |c_s|^2 &= \frac{|\varepsilon_l|^2}{\kappa^2 + \Delta^2}, \end{aligned} \quad (5)$$

with $\Delta = \Delta_c - \chi q_s / \hbar$, and the solution of c_+ [22] is

$$c_+ = \frac{(\delta^2 - \omega_m^2 + i\gamma_m \delta)[\kappa - i(\Delta + \delta)] - 2i\omega_m \beta}{[\Delta^2 + (\kappa - i\delta)^2](\delta^2 - \omega_m^2 + i\delta\gamma_m) + 4\Delta\omega_m \beta} \quad (6)$$

with $\beta = \chi^2 |c_s|^2 / (2m\hbar\omega_m)$.

Making use of the input-output relation of the cavity [38], we have the output field

$$\begin{aligned} \varepsilon_{out} &= \varepsilon_{in} - 2\kappa c \\ &= \varepsilon_l + \varepsilon_p e^{-i\delta t} - 2\kappa(c_s + c_+ \varepsilon_p e^{-i\delta t} + c_- \varepsilon_p^* e^{i\delta t}), \end{aligned} \quad (7)$$

and thereby the transmission of the probe field is given by [23]

$$t_p = \frac{\varepsilon_p - 2\kappa \varepsilon_p c_+}{\varepsilon_p} = 1 - 2\kappa c_+, \quad (8)$$

which can be measured by homodyne technique [38].

Defining $\varepsilon_T = 2\kappa c_+$, we obtain the quadrature ε_T of the optical components with frequency ω_p in the output field,

$$\varepsilon_T = 2\kappa \frac{(\delta^2 - \omega_m^2 + i\gamma_m \delta)[\kappa - i(\Delta + \delta)] - 2i\omega_m \beta}{[\Delta^2 + (\kappa - i\delta)^2](\delta^2 - \omega_m^2 + i\delta\gamma_m) + 4\Delta\omega_m \beta}, \quad (9)$$

whose real and imaginary parts, $\text{Re}[\varepsilon_T]$ and $\text{Im}[\varepsilon_T]$, represent the absorptive and dispersive behavior of the optomechanical system, respectively [22].

In order to reduce Eq. (9) and understand the relationship between the charge number and the OMIT, we assume following conditions [22, 23]: (i) $\Delta \simeq \omega_m$ and (ii) $\omega_m \gg \kappa$. The first condition means the frequency of the cavity to be resonant with that of the optomechanical anti-Stokes sideband, which actually leads to optimal cooling. The second condition is the well-known resolved sideband condition, which ensures the OMIT splitting to be distinguished [23]. Moreover, it is known that the coupling between the MR and the cavity is strongest in the case of $\delta \simeq \omega_m$ [22], which makes $\delta^2 - \omega_m^2 \simeq 2\omega_m(\delta - \omega_m)$ achievable. Under these conditions, we rewrite the output field as

$$\varepsilon_T \approx \frac{2\kappa}{\kappa - i(\delta - \omega_m) + \frac{\beta}{\frac{\gamma_m}{2} - i(\delta - \omega_m)}}. \quad (10)$$

Compared with the expression of the output field in Eq. (7) in Ref. [22], the parameter β in Eq. (10) in our case is modified to be a function of the charge number n . Under appropriate conditions, the window width of the OMIT can be used to identify the charge number of the charged body.

IV. THE CHARGE NUMBER AND THE OUTPUT FIELD

We show below in details how the charge number impacts the mean photon number and how to measure the charge number by the window width of the OMIT.

From Eq. (5), we have a third-order nonlinear equation for the MR position q_s ,

$$aq_s^3 + bq_s^2 + fq_s + d = 0, \quad (11)$$

with

$$\begin{aligned} a &= m\omega_m^2 \frac{\chi^2}{\hbar^2}, \\ b &= -2m\omega_m^2 \frac{\chi}{\hbar} (\Delta_c) - n\eta \frac{\chi^2}{\hbar^2}, \\ f &= m\omega_m^2 \kappa^2 + m\omega_m^2 (\Delta_c)^2 + 2n\eta (\Delta_c) \frac{\chi}{\hbar}, \\ d &= -n\eta \kappa^2 - n\eta (\Delta_c)^2 - \chi |\varepsilon_l|^2. \end{aligned} \quad (12)$$

To get a more intuitive understanding of the role that the Coulomb interaction plays in Eqs. (9) and (10), we suppose $n\eta \gg \chi |c_s|^2$, and obtain the solutions to Eq. (11) as

$$q_s = \begin{cases} \chi |c_{s0}|^2 / (m\omega_m^2), & (n = 0) \\ n\eta / (m\omega_m^2), & (n \geq 1) \end{cases} \quad (13)$$

with $|c_{s0}|^2$ being the mean photon number in absence of the Coulomb interaction between the MR and charged

object. The above equation means that, for no charge in the system, the MR has a steady-state position $q_s = \chi|c_{s0}|^2/(m\omega_m^2)$ under the action of pumping field. In the presence of the attractive Coulomb interaction between the charged body and the MR, the steady-state position of the MR is modified. In the case of $n\eta \gg \chi|c_s|^2$, the steady-state position $q_s = n\eta/(m\omega_m^2)$ reduces to a function of charge number in the object. The phenomena have been shown in Fig. 2(a).

Moreover, from Eqs. (5) and (13), the mean photon number takes the form of

$$|c_s|^2 = \begin{cases} |c_{s0}|^2, & (n = 0) \\ \frac{|\varepsilon_l|^2}{\kappa^2 + (\Delta_c - \frac{\chi n\eta}{\hbar m\omega_m^2})^2}, & (n \geq 1) \end{cases} \quad (14)$$

which implies that the photon number increases (decreases) with the charge number for $\Delta_c \geq \chi q_s/\hbar$ ($\Delta_c < \chi q_s/\hbar$) in the case of the fixed pumping field. So there should be a maximal photon number with respect to the change of the charge number, as demonstrated in Fig. 2(b).

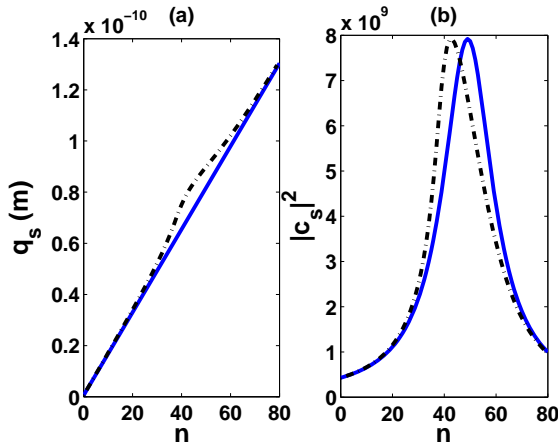


FIG. 2: (Color online) (a) The position q_s versus the charge number n ; (b) The mean photon number as a function of the charge number n . The black dotted-dashed lines [blue solid lines] represent the exact values [the approximate values] of q_s and $|c_s|^2$ using Eq. (11) and Eq. (5) [Eq. (13) and Eq. (14)], respectively. The values are taken from the experiments in Refs. [4, 5, 22, 39–41] as $k = 8.897\text{N}\cdot\text{m}^2/\text{C}^2$, $\lambda_c \equiv 2\pi c/\omega_c = 1064$ nm, $L = 25$ mm, $m = 145$ ng, $\kappa = 2\pi \times 215$ kHz, $\omega_m = 2\pi \times 947$ kHz, $\gamma_m = 2\pi \times 141$ Hz, $r_0 = 67$ μm , $\varepsilon_l = \sqrt{2P\kappa/\hbar\omega_c}$ with $P = 1$ mW, $Q_{MR} = CU$, $C = 27.5$ nF and $U = 1$ V.

In Fig. 2, the black dotted-dashed and blue solid lines correspond to the steady-state position and the mean photon number without and with the approximate condition $n\eta \gg \chi|c_s|^2$, respectively, as functions of the charge number. The steady-state position increases monotonously with the charge number, while the mean photon number is a pulse-like curve. In the scope of charge number from 30 to 55, there is a little difference

between the exact values and approximate values of both q_s and $|c_s|^2$. This deviation results from the fact that the approximate condition $n\eta \gg \chi|c_s|^2$ is not satisfied very well for the mean photon number $|c_s|^2 \simeq 0.3n\eta/\chi$ in this scope. Within the region of $n \leq 40$, the slight difference between the exact and approximate values implies our assumption $n\eta \gg \chi|c_s|^2$ to be reasonable for the parameters we considered in Fig. 2. In this region, both the mean photon number and the MR deformation are ultra-sensitive to the charge number in a monotonous way, and thereby the charge number less than 40 can be fully characterized by the window width of the OMIT.

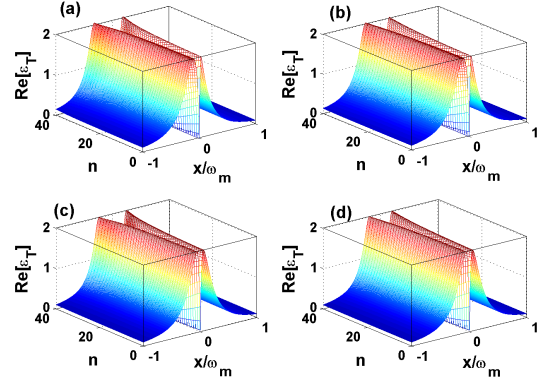


FIG. 3: (Color online) The real part of the output $Re[\varepsilon_{out}]$ (the absorption) versus the charge number n and the detuning $x = \delta - \omega_m$, where (a) and (b) are the exact values calculated from Eq. (9). (c) and (d) are the approximate values using Eq. (10). The parameter values are the same as in Fig. 2.

To show this point more clearly, we have simulated the real part of the output field using Eq. (9) and Eq. (10) for $n \leq 40$ (see Fig. 3). Compared with the exact results, the simplified expression of the output field Eq. (9) is justified. Moreover, from Fig. 3, we see that the absorption vanishes at $x = 0$ (i.e., $\delta = \omega_m$) and the window width of the OMIT increases with the charge number n . So we are able to detect the charge number of a nearby charged object by the OMIT. In addition, in our case with $n = 0$, the values in the figure can be straightforwardly reduced to those of non-charge case as in Ref. [22].

For clarifying the efficiency and the effect of our scheme, we consider a fixed charge number n in the charged object. There are three tuning points in the real part of the output field versus the detuning $x = \delta - \omega_m$,

$$\begin{cases} x_{\pm} = \pm \sqrt{\frac{\sqrt{2}(2\kappa + \gamma_m)\sqrt{\beta(2\beta + \kappa\gamma_m)} - \gamma_m(2\beta + \kappa\gamma_m)}{4\kappa}} \\ x_0 = 0 \end{cases}, \quad (15)$$

which can be obtained by solving $d\varepsilon_T/dx = 0$. Excluding the trivial case of $x_0 = 0$ and considering the symmetry of x_+ and x_- , we take the tuning point x_+ as an example

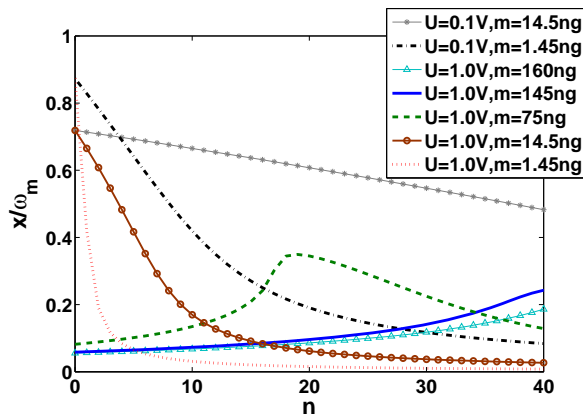


FIG. 4: (Color online) The detuning x for tuning point versus the charge number n . Except the values in the inset, other parameter values are the same as in Fig. 2.

in Fig. 4 for different masses and charges. Since the parameters used in Fig. 4 satisfy $2\beta \gg \kappa\gamma_m$, we may reduce Eq. (15) to $x_+ \sim \sqrt{\beta}$. Therefore, by changing the MR's effective mass m and the MR's charge Q_{MR} , we present three typically different relationships between the detuning x_+ and the charge number n : (1) The monotonous increase (i.e., the gray asterisk and blue solid curves); (2) The monotonous decrease (i.e., the red dotted and the black dotted-dashed curves); (3) The curve with a hump in the middle (i.e., the green dashed curve). The curves indicate that the heavy (light) MR is suitable for detecting large (small) charge numbers. In addition, although the MR with intermediate mass seems useless in our scheme, the charge number before the hump ($n < 18$) in Fig. 4 can still be used to detect the charge number. Moreover, for the same mass of the MR, the lower the applied voltage, the less tilting the curve in Fig. 4. As a result, to detect more precisely the tiny charge, e.g., a single charge, we should increase the voltage to obtain more precise resolution.

V. CONCLUSION

We would like to point out that the analytical solutions to our detection scheme are based on some approximations ($n\eta \gg \chi|c_s|^2$ and $\delta \sim \omega_m$), which have been justified by numerical calculation with the parameter values we used. It has been shown that the MR with an ef-

fective mass of 1.45 ng and a voltage of 0.1 V is more suitable than others to measure the small charge number (see black dotted-dashed curves in Fig. 4). Experimentally, the effective mass of a MR as small as 50 pg has been achieved [15]. So we may expect to have better detection with the MRs of such small effective masses.

In addition, from the parameters for the curves in Fig. 4, we can infer the minimal Coulomb force detected by our scheme, which is $F = k \frac{Q_{MR}|e|}{r^2} = 0.88$ nN, much weaker than the minimal electrical gradient force $F_{grad} = 0.4$ μ N in [34, 35], but larger than the tiny force $F_{min} = 53$ aN detectable in Ref. [36]. Nevertheless, our scheme focuses on the detection of charge number, rather than the force. Moreover, the highest sensitivity of the surface charge density in our scheme is about $1/(0.1r_0)^2 \simeq 2.2 \times 10^6$ cm^{-2} , which is of the same order as the one (6.25×10^6 cm^{-2}) in Ref. [42]. The sensitivity in our case can be further enhanced by increasing the bias gate voltage or decreasing the mass of the MR.

In summary, we have demonstrated how to realize precision measurement of small charge number of the charged object via monitoring the OMIT in optomechanical system in the presence of the Coulomb interaction between the charged MR and the object. From the analytical relationship we obtained for the OMIT window width with the charge number in a small charged body, we have shown the possibility of detecting few charges (even a single charge) from the output spectra of the OMIT. The feasibility of our proposal has been assessed by using currently available parameters, and the Coulomb attraction under our consideration can be straightforwardly extended to Coulomb repulsion. We believe that the proposal would be helpful for exploring quantum behavior in MRs and for precision measurement using OMIT.

Acknowledgments

We would like to thank G. S. Agarwal, and Sumei Huang for helpful discussions. The work is supported by National Fundamental Research Program of China (Grant Nos. 2012CB922102, 2012CB922104, 2009CB929604 and 2007CB925204), National Natural Science Foundation of China (Grant Nos. 60978009 and 11174027), and Research Funds of Renmin University of China (Grant No. 10XNL016).

-
- [1] V. B. Braginsky and A. B. Manukin, *Measurements of Weak Forces in Physics Experiments* (Chicago University Press, Chicago, 1977).
 [2] L. F. Wei, Y. X. Liu, C. P. Sun, F. Nori, Phys. Rev. Lett. **97**, 237201 (2006).
 [3] F. Marquardt, and S. M. Girvin, Physics **2**, 40 (2009).
 [4] S. Groblacher, K. Hammerer, M. Vanner, and M. Asp-

- elmeyer, Nature (London) **460**, 724 (2009).
 [5] J. D. Thompson, B. M. Zwickl, A. M. Jayich, F. Marquardt, S. M. Girvin, and J. G. E. Harris, Nature (London) **452**, 72 (2008).
 [6] Y. Li, Y. D. Wang, F. Xue, and C. Bruder, Phys. Rev. B **78**, 134301 (2008).
 [7] I. Wilson-Rae, P. Zoller, and A. Imamoglu, Phys. Rev.

- Lett. **92**, 075507 (2004).
- [8] I. Wilson-Rae, N. Nooshi, W. Zwerger, and T. J. Kippenberg, Phys. Rev. Lett. **99**, 093901 (2007).
- [9] F. Marquardt, J. P. Chen, A. A. Clerk, and S. M. Girvin, Phys. Rev. Lett. **99**, 093902 (2007).
- [10] P. Zhang, Y. D. Wang, and C. P. Sun, Phys. Rev. Lett. **95**, 097204 (2005).
- [11] K. Xia and J. Evers, Phys. Rev. Lett. **103**, 227203 (2009).
- [12] Y. Li, L. A. Wu, Y. D. Wang, and L. P. Yang, Phys. Rev. B **84**, 094502 (2011).
- [13] A. Mari and J. Eisert, Phys. Rev. Lett. **108**, 120602 (2012).
- [14] C. H. Metzger and K. Karrai, Nature (London) **432**, 1002 (2004).
- [15] S. Groblacher *et al.*, Nat. Phys. **5**, 485 (2009).
- [16] T. Rocheleau *et al.*, Nature (London) **463**, 72 (2010).
- [17] J. D. Teufel, T. Donner, D. Li, J. W. Harlow, M. S. Allman, K. Cicak, A. J. Sirois, J. D. Whittaker, K. W. Lehnert, and R. W. Simmonds, Nature (London) **475**, 359 (2011).
- [18] J. Chan, T. P. M. Alegre, A. H. Safavi-Naeini, J. T. Hill, A. Krause, S. Groblacher, M. Aspelmeyer, and O. Painter, Nature (London) **478**, 89 (2011).
- [19] A. D. O'Connell, M. Hofheinz, M. Ansmann, R. C. Bialczak, M. Lenander, E. Lucero, M. Neeley, D. Sank, H. Wang, M. Weides, J. Wenner, J. M. Martinis, and A. N. Cleland, Nature (London) **464**, 697 (2010).
- [20] A. Schliesser, O. Arcizet, R. Riviere, G. Anetsberger, and T. J. Kippenberg, Nat. Phys. **5**, 509 (2009).
- [21] P. Verlot, A. Tavernarakis, T. Briant, P.-F. Cohadon, and A. Heidmann, Phys. Rev. Lett. **104**, 133602 (2010).
- [22] G. S. Agarwal and S. Huang, Phys. Rev. A **81**, 041803 (2010).
- [23] S. Weis, R. Riviere, S. Deleglise, E. Gavartin, O. Arcizet, A. Schliesser, and T. J. Kippenberg, Science **330**, 1520 (2010).
- [24] H. Xiong, L. G. Si, A. S. Zheng, X. Yang and Y. Wu, Phys. Rev. A **86**, 013815 (2012).
- [25] Q. Lin, J. Rosenberg, D. Chang, R. Camacho, M. Eichenfield, K. J. Vahala, and O. Painter, Nat. Photon. **4**, 236 (2010).
- [26] A. H. Safavi-Naeini, T. P. M. Alegre, J. Chan, M. Eichenfield, M. Winger, Q. Lin, J. T. Hill, D. Chang, and O. Painter, Nature (London) **472**, 69 (2011).
- [27] J. D. Teufel, D. Li, M. S. Allman, K. Cicak, A. J. Sirois, J. D. Whittaker, and R. W. Simmonds, Nature (London) **471**, 204 (2011).
- [28] G. S. Agarwal and S. Huang, Phys. Rev. A **85**, 021801 (2012).
- [29] S. Forstner, S. Prams, J. Knittel, E. D. van Ooijen, J. D. Swaim, G. I. Harris, A. Szorkovszky, W. P. Bowen, and H. Rubinsztein-Dunlop, Phys. Rev. Lett. **108**, 120801 (2012).
- [30] K. L. Ekinci, Small **1**, 786 (2005).
- [31] G. Rietveld, IEEE T. Instrum. Meas. **56**, 559 (2010).
- [32] E. Lamminen, J. Phys. Conf. **304**, 012064 (2011).
- [33] C. Xiong, X. Sun, K. Y. Fong, and H. X. Tang, Appl. Phys. Lett. **100**, 171111 (2012).
- [34] K. H. Lee, T. G. McRae, G. I. Harris, J. Knittel, and W. P. Bowen, Phys. Rev. Lett. **104**, 123604 (2010).
- [35] T. G. McRae, K. H. Lee, G. I. Harris, J. Knittel, and W. P. Bowen, Phys. Rev. A **82**, 023825 (2010).
- [36] H. Miao, K. Srinivasan, and V. Aksyuk, New J. Phys. **14**, 075015 (2012).
- [37] S. Huang and G. S. Agarwal, Phys. Rev. A **83**, 023823 (2011).
- [38] D. F. Walls and G. J. Milburn, *Quantum Optics* (Springer-Verlag, Berlin, 1994).
- [39] M. LaHaye, O. Buu, B. Camarota, and K. Schwab, Science **304**, 74 (2004).
- [40] W. K. Hensinger, D. W. Utami, H.-S. Goan, K. Schwab, C. Monroe, and G. J. Milburn, Phys. Rev. A **72**, 041405 (2005).
- [41] J. C. Sankey, C. Yang, B. M. Zwickl, A. M. Jayich, and J. G. E. Harris, Nat. Phys. **6**, 707 (2010).
- [42] X. Shan, X. Huang, K. J. Foley, P. Zhang, K. Chen, S. Wang, and N. Tao, Anal. Chem. **82**, 234 (2010).